Biogeosciences
Open Access

Discussions

Technical Note: A simple calculation algorithm to separate high-resolution CH$_4$ flux measurements into ebullition and diffusion-derived components

M. Hoffmann[1], M. Schulz-Hanke[2], J. Garcia Alba[1], N. Jurisch[2], U. Hagemann[2], T. Sachs[3], M. Sommer[1,4], and J. Augustin[2]

[1]Institute of Soil Landscape Research, Leibniz Centre for Agricultural Landscape Research (ZALF), Eberswalder Str. 84, 15374 Müncheberg, Germany
[2]Institute for Landscape Biogeochemistry, Leibniz Centre for Agricultural Landscape Research (ZALF), Eberswalder Str. 84, 15374 Müncheberg, Germany
[3]GFZ German Research Centre for Geosciences, Telegrafenberg, 14473 Potsdam, Germany
[4]University of Potsdam, Institute of Earth and Environmental Sciences, Karl-Liebknecht-Str. 24–25, 14476 Potsdam, Germany

Correspondence to: M. Hoffmann (mathias.hoffmann@zalf.de)

Discussion Paper | Discussion Paper | Discussion Paper | Discussion Paper |

BGD

12, 12923–12945, 2015

Technical Note: A simple calculation algorithm to separate high-resolution

M. Hoffmann et al.

Title Page

Abstract | Introduction

Conclusions | References

Tables | Figures

|◄ | ►|

◄ | ►

Back | Close

Full Screen / Esc

Printer-friendly Version

Interactive Discussion

Technical Note: A simple calculation algorithm to separate high-resolution

M. Hoffmann et al.

Abstract

Processes driving the production, transformation and transport of methane (CH_4) in wetland ecosystems are highly complex. Thus, serious challenges are constitutes in terms of the mechanistic process understanding, the identification of potential environmental drivers and the calculation of reliable CH_4 emission estimates. We present a simple calculation algorithm to separate open-water CH_4 fluxes measured with automatic chambers into diffusion- and ebullition-derived components, which helps facilitating the identification of underlying dynamics and potential environmental drivers. Flux separation is based on ebullition related sudden concentration changes during single measurements. A variable ebullition filter is applied, using the lower and upper quartile and the interquartile range (IQR). Automation of data processing is achieved by using an established R-script, adjusted for the purpose of CH_4 flux calculation. The algorithm was tested using flux measurement data (July to September 2013) from a former fen grassland site, converted into a shallow lake as a result of rewetting ebullition and diffusion contributed 46 and 55 %, respectively, to total CH_4 emissions, which is comparable to those previously reported by literature. Moreover, the separation algorithm revealed a concealed shift in the diurnal trend of diffusive fluxes throughout the measurement period.

1 Introduction

Wetlands and freshwaters are among the main sources for methane (CH_4) emissions (Dengel et al., 2013; Bastviken et al., 2011; IPCC 2007). In open-water systems, CH_4 is released via three pathways: (i) diffusion, (ii) ebullition and (iii) plant mediated transport (e.g., Goodrich et al., 2011; Bastviken et al., 2004; Van der Nat and Middelburg, 2000; Whiting and Chanton, 1996), which are all subject to variable environmental drivers and conditions such as water level, atmospheric pressure, temperature gradients, and wind velocity as well as the presence of macrophytes (Lai et al., 2012;

Tokida et al., 2007; Chanton and Whiting, 1995). As the absolute and relative contributions of these pathway-associated flux components varies in time and space (Maeck et al., 2013; Walter et al., 2006), the resulting total CH_4 emissions feature an extremely high spatial and temporal variability at all scales (Koch et al., 2014; Repo et al., 2007;

5 Bastviken et al., 2004). Hence, attempts to model CH_4 emissions based on individual environmental drivers are highly complex and complicated (Prairie and del Giorgio, 2013). The separation of measured CH_4 emissions into the individual pathway-associated components is therefore crucial if aiming to identify relevant environmental drivers of CH_4 emissions (Bastviken et al., 2011, 2004). In consequence, the under-

10 standing of the complex processes determining the temporal as well as spatial patterns of CH_4 emissions is a prerequisite for upscaling field-measured CH_4 emissions to the regional or landscape scale, and thus for adequately quantifying the contribution of CH_4 emissions to global greenhouse gas (GHG) budgets (Walter et al., 2015; Koebsch et al., 2015; Lai et al., 2012; Limpens et al., 2008).

15 However, field studies measuring emitted CH_4 above the water surface generally measure the total CH_4 emissions as a mixed signal of individual CH_4 emission components, released via all possible pathways (i.e. diffusion, ebullition and plant mediated transport). Studies directly measuring temporal and spatial patterns of CH_4 emissions resulting only from either ebullition or diffusion are rare. Measurements of CH_4 ebul-

20 lition can be performed using manual or automatic gas traps, as well as optical and hydroacoustic methods (Wik et al., 2011, 2013; Maeck et al., 2013; Walter et al., 2008; Ostrovsky et al., 2008; Huttunen et al., 2001; Chanton and Whiting, 1995), often requiring a certain degree of manipulation of the studied system. Diffusive CH_4 fluxes are commonly either derived indirectly as the difference between total CH_4 emissions and

25 measured ebullition, or directly obtained based on the use of bubble shields or gradient measurements of CH_4 concentration differences (DelSontro et al., 2011; Bastviken et al., 2010, 2004). A graphical method to separate diffusion, steady ebullition and episodic ebullition fluxes from the total CH_4 flux was presented by Yu et al. (2014), using a flow-through chamber system. However, performed at the laboratory scale for

a peat monolith, measurement results, as well as the applied method, were lacking direct field applicability. A first simple mathematical approach for field measurements to separate ebullition from the sum of diffusion and plant mediated transport was introduced by Miller and Oremland (1988), who used low resolution static chamber measurements. Goodrich et al. (2011) specified the approach using piecewise linear fits for single ebullition events. However, static thresholds determining ebullition events, as well as low-resolution measurements, limited the approach to estimates of medium and major ebullition events and prevent a clear flux separation.

CH_4 flux separation approaches based on manual chamber measurements with rather low temporal resolution fail to capture the rapidly changing absolute and relative contributions of the pathway-associated flux components both in time and space (Maeck et al., 2013; Walter et al., 2006). Improvements in measurement techniques, particularly by using micrometeorological methods (e.g., Eddy Covariance (EC)), however, allowed for high temporal resolution records of CH_4 emissions (Juszczak and Augustin, 2013; Schrier-Uijl et al., 2011; Cole et al., 2010; Wille et al., 2008). Recently, a growing number of experimental GHG studies employ automatic chambers (AC) (Koskinen et al., 2014; Lai et al., 2014), which can also provide flux data with an enhanced temporal resolution capturing short-term temporal (e.g. diurnal) dynamics. In addition, AC measurements can also represent small-scale spatial variability, and thus, identify potential hot spots of CH_4 emissions (Koskinen et al., 2014; Lai et al., 2014). AC systems combine the advantages of chamber measurements and micrometeorological methods with respect to the quantification of spatial as well as temporal dynamics of CH_4 emissions (Savage et al., 2014; Lai et al., 2012).

Moreover, there is a need for a non-intrusive method for separating pathway-associated CH_4 flux components both in time and space. Due to the combination high temporal measurement resolution and representation of small-scale spatial heterogeneity, AC measurements provide opportunities for (i) detecting even minor ebullition events and (ii) developing a statistically based flux separation approach. Based on high-resolution CH_4 flux data from an AC measurement system, this study presents

a new calculation algorithm for separating open-water CH_4 fluxes into its ebullition- and diffusion-derived components based on ebullition-related sudden concentration changes during chamber closure. A variable ebullition filter is applied, using the lower and upper quartile and the interquartile range (IQR). Data processing is based on the R-script developed by Hoffmann et al. (2015), modified for the purpose of CH_4 flux calculation and separation, thus including the advantages of automated and standardized flux estimation. We hypothesize that the presented flux calculation and separation algorithm can reveal concealed spatial and temporal dynamics in ebullition and diffusion-associated CH_4 fluxes, thus, facilitating the identification of relevant environmental drivers.

2 Material and methods

2.1 Exemplary field data

2.1.1 Study site

Ecosystem CH_4 exchange was measured at a rewetted former fen grassland site, located within the Peene river valley in Mecklenburg-Western Pomerania, northeast Germany (53°52′ N, 12°52′ E). The long-term annual precipitation is 570 mm. The mean annual air temperature is 8.7 °C (DWD, Anklam). The study site was particularly influenced by a complex melioration and drainage program between 1960 and 1990, characterized by intensive agriculture. As a consequence, the peat layer was degraded and the soil surface was lowered by subsidence. Being included in the Mecklenburg-Western Pomerania Mire Restoration Program, the study site was rewetted at the beginning of 2005, resulting in a water level permanently above the soil surface, thus, transforming the site into a shallow lake. Exceptionally high CH_4 emissions at the measurement site are reported by Hahn-Schöffl et al. (2011), who investigated sediments formed during inundation. Prior to rewetting, the vegetation was dominated by reed

canary grass (*Phalaris arundinacea*), which disappeared after rewetting due to the higher ground water level. At present, the water surface is partially covered with duckweed (*Lemna*), while bulrush (*Typha*) and swamp grass (*Glyceria*) are present next to the shoreline. However, below chambers, no emergent macrophytes were present throughout the study period.

2.1.2 Automatic chamber system

In April 2013, the measurement site was equipped with an AC system and a nearby climate station (Fig. 1). The AC system consists of four transparent chambers, installed along a transect directed from the shoreline into the lake. Chambers are made of Lexan Polycarbonate with a thickness of 2 mm and reinforced by an aluminium frame. Each chamber (volume of 1.5 m^3 ; base area 1 m^2) is mounted in a steel profile, secured by wires, and lifted/lowered by an electronically controlled cable winch, located at the top of the steel profile. All chambers are equipped with a water sensor (capacitive limit switch KB 5004, efector150) at the bottom, which allows steady immersion (5 cm) of the chambers into the variable water surface. Hence, airtight sealing, as well as constant chamber volume are ensured during the study period. Chambers are connected by two tubes and a multiplexer to a single Los Gatos Fast Greenhouse Gas Analyser (911-0010, Los Gatos), measuring the air concentration of carbon dioxide (CO_2), methane (CH_4), and water vapor (H_2O). To ensure consistent air pressure and mixture during measurements, chambers are ventilated by a fan and sampled air is transferred back into the chamber headspace. However, due to the big chamber volume, mixture of the chamber headspace needed up to 30 s, wherefore most peaks due to ebullition events showed overcompensation (Fig. 3). Concentration measurements are performed in sequence, sampling each chamber for 10 min with a 15 s frequency once an hour. A wooden boardwalk north of the measurement site allows for maintenance access, while avoiding disturbances of the water body and peat surface.

Technical Note: A simple calculation algorithm to separate high-resolution

M. Hoffmann et al.

2.1.3 Ancillary field measurements

Temperatures were recorded in different water (5 cm above soil surface) and soil/sediment depths (2, 5, 10 cm below sediment–water interface), using thermocouples (T107, Campbell Scientific). Additionally, air temperature in 20 and 200 cm height,
5 as well as wind speed, wind direction, precipitation, relative humidity, and air pressure were measured by a nearby climate station (WXT52C, Vaisala). Information about the water table depth was gained by a pressure probe (PDCR1830, Campbell Scientific). All parameters were continuously recorded at 30 min intervals and stored by a data logger (CR 1000, Campbell Scientific) connected to a GPRS radio modem.

2.2 Flux calculation and separation algorithm

CH_4 flux calculation was performed using a standardized R-script presented in detail by Hoffmann et al. (2015). Measured fluxes were determined using Eq. (1), where M is the molar mass of CH_4, δv is the linear concentration change over time (t), A and V denote the basal area and chamber volume, respectively, and T and P represent the
15 inside air temperature and air pressure. R is a constant ($8.3143\,\mathrm{m^3\,Pa\,K^{-1}\,mol^{-1}}$).

$$rCH_4(\mu mol\,C\,m^{-2}s^{-1}) = \frac{M \times P \times V \times \delta v}{R \times T \times t \times A} \qquad (1)$$

To estimate the relative contribution of diffusion and ebullition to total CH_4 emissions, flux calculation was performed twice, adjusting selected user-defined parameter setups of the used R-script (Hoffmann et al., 2015) (Fig. 3). First, the diffusive component of
20 the flux rate ($CH_{4diffusion}$) was calculated, based on a variable moving window (MW) with a minimum size of 5 consecutive data points. Abrupt concentration changes within the MW were identified by means of a rigid outliner test, discarding fluxes with an inherent concentration change bigger or lower than the upper and lower quartile ±0.25 times the interquartile range (IQR). Tests of variance homogeneity and normal distribution
25 were applied with $\alpha = 0.1$. Second, the total CH_4 flux (CH_{4total}) for each measurement

was calculated as the difference between the start and end CH_4 concentration, using an enlarged MW with a minimum length of 7.5 min. To avoid measurement artefacts (e.g. overcompensation), being taken into account as start or end concentration, measurement points representing an inherent concentration change lower or bigger than the upper and lower quartile ±0.25 times IQR, were discarded prior to calculation of the total CH_4 flux. Third, the proportion of the total CH_4 emission, released via ebullition, was estimated following Eq. (2).

$$CH_{4\,ebullition\,n} = \sum_{i=1}^{n} \left(CH_{4\,total} - CH_{4\,diffusion} \right) \qquad (2)$$

Since no emergent macrophytes were present below the automatic chambers, plant mediated transport of CH_4 was assumed to be zero. In case of negative estimates, CH_4 emission, due to ebullition, was assumed to be zero. To exclude measurement artefacts, triggered by the process of closing the chamber, a death band of 25 % was applied to the beginning of each measurement prior to all flux calculation steps. The used R-script is available at www.carbozalf.org.

2.3 Verification of applied flux separation algorithm

A laboratory experiment under reasonable controlled conditions was performed, to verify the used flux separation algorithm. Therefore, distinct amounts (5, 10, 20, 30 and 50 mL) of a gaseous mixture (25 000 ppm CH_4 in artificial air; Linde, Germany) were inserted by a syringe through a pipe into a water filled tub, covered with a closed chamber ($V = 0.114\ m^3$; $A = 0.145\ m^2$). Airtight sealing was ensured by a water filled frame, connecting tub and chamber. The chamber was ventilated by a fan and connected via pipes to a Los Gatos Greenhouse Gas Analyser (911-0010, Los Gatos), measuring CH_4 concentrations inside the chamber with a 1 Hz frequency (Fig. 2). In terms of comparability between in vitro and in situ measurements, data processing was performed based on 0.066 Hz records. Expected concentration changes within chamber headspace as the

result of methane injections were calculated as mixing ratio between the amount of inserted gaseous mixture (25 000 ppm) and air filled chamber volume (2 ppm).

3   Results and discussion

The assumption of using sudden changes in chamber based CH_4 concentrations mea-
surements for detecting ebullition events was verified by the conducted lab experiment. Calculations of simulated ebullition events and the amount of injected CH_4 showed a well overall agreement, which indicates the accuracy of the calculation algorithm (Fig. 4). However, flux separation might be hampered due to a steady flux originating from other processes than diffusion through peat and water layers, such as steady ebullition of micro bubbles (Goodrich et al., 2011). A resulting potential impact on es-timates of diffusive CH_4 emissions can be minimized by an enhanced frequency of concentration measurements during chamber closure. Based on a high temporal reso-lution small-scale differences within measured concentration changes can be identified and filtered by the variable IQR-criterion, which thereby reduces the detection limit of ebullition events. Compared to direct measurements of either diffusion or ebullition, as reported by e.g. Bastviken et al. (2010), the presented calculation algorithm prevents an interfering influence of spatial heterogeneity on separated ebullition and diffusion CH_4 fluxes, since both flux components are derived during the same measurement. Moreover, the integration of the ebullition component over measurements rather than the calculation of single ebullition events are ensuring a reliable flux separation despite of potential measurement artefacts such as overcompensation or incomplete ebullition records (Goodrich et al., 2011; Miller and Oremland, 1988). In case of a low water level, such as within the presented study (< 35 cm) or parallel measurements of differ-ent trace gases (e.g. CO_2 and CH_4), the use of direct measurement systems for either ebullition (gas traps, funnels) or diffusion (bubble shields) might be limited. Hence, the presented simple and robust calculation algorithm as purely data processing based

seems to be applicable for a broader range of different manual and automatic closed chamber systems, setups and ecosystems.

Due to the performed flux separation, the accuracy of certain spatial and temporal tendencies within the exemplary field data set was improved (Fig. 4 and Table 1) and explanatory approaches could be addressed. Total CH_4 emissions spatially integrated over the study period, as well as the respective contributions of ebullition and diffusion are shown in Fig. 4. Apart from short-term measurement gaps, a considerable loss of data occurred between the 27 July and 7 August 2013, due to malfunction of the measurement equipment. In general, biochemical processes driving CH_4 production are closely related to temperature regimes (Christensen et al., 2005), determining the CH_4 production within the sediment (Bastviken et al., 2004). Hence, measured total CH_4 emissions showed clear seasonal patterns, following the temperature regime at 10 cm soil depth. In addition to seasonality, total CH_4 emissions also featured diurnal dynamics, with lower fluxes during daytime and higher fluxes during nighttime, which were most pronounced during July and early September. Especially during August, the diurnal variability was superimposed by short-term emission events and high amplitudes in recorded total CH_4 emissions. Similar to the total CH_4 emissions, also diffusive fluxes showed a distinct temperature-driven seasonality, as well as clear diurnal patterns throughout the entire study period. However, compared to diurnal variability of the total CH_4 fluxes, a pronounced shift of maximum CH_4 emissions from night- to daytime was revealed for the diffusive flux component (Fig. 5). While maximum diffusive fluxes during July were recorded at nighttime hours (approx. 19:00 to 7:00 LT), a shift to the daytime started in August, with maximum fluxes in September occurring between 2:00 and 14:00 LT. This might be explained by differences in turbulent mixing, due to certain water temperature gradients. During daytime, the surface water is warmed, preventing an exchange with the CH_4 enriched water next to the sediment, which results in lower diffusive CH_4 emissions. During nighttime, when the upper water layer cools down and intermix is undisturbed, enhanced diffusive CH_4 emissions can be detected. This dynamics are more pronounced during warm days, explaining the

seasonal shift and concealed during periods with a high wind velocity. The obtained diurnal trend is in accordance with findings of Sahlée et al. (2014) and Lai et al. (2012), who reported higher nighttime and lower daytime CH_4 emissions for a lake site in Sweden and an ombrothropic bog in Canada, respectively. However, an opposing tendency was found by Deshmukh et al. (2014), who reported higher daytime and lower nighttime CH_4 emissions from a newly flooded subtropical freshwater hydroelectric reservoir within the Lam Theun river valley, Laos. In contrast to diurnal trends obtained for the total as well as diffusive CH_4 emissions, estimated ebullition events occurred erratically and neither showed clear seasonal nor diurnal dynamics. Nonetheless, periods characterized by more pronounced ebullition, seemed to roughly follow soil temperature-driven CH_4 production within the sediment as e.g. reported by Bastviken et al., 2004 (Fig. 5). This is confirmed by a distinct correlation between daily mean soil temperatures and corresponding sums of measured ebullition fluxes. Moreover, fewer and smaller ebullition events were detected in times of reduced wind velocity and high relative humidity (RH), for example from 10–11 September and 18–19 September 2013. However, on the level of single flux measurement, no significant dependency between recorded environmental drivers and CH_4 release by ebullition events was found. The relative contribution of diffusion and ebullition was 55 % (min. 33 to max. 70 %) and 46 % (min. 30 to max. 67 %), respectively. This is in accordance with values, reported by Bastviken et al. (2011), who compiled CH_4 emission estimates from 474 freshwater ecosystems with clearly defined emission pathways. A similar ratio was also found by Tokida et al. (2007), who investigated the role of decreasing atmospheric pressure as a trigger for CH_4 ebullition events in peatlands.

Comparison of flux data among the four chambers, reveals considerable spatial heterogeneity within the measured transect (data not shown). Monthly averages of diffusive, ebullative and total CH_4 emissions for all four chambers of the established transect, as well as statistics, showing the explanatory power of different environmental variables, are summarized in Table 1. Separated into diffusion and ebullition, different tendencies along the transect, as well as dependencies from different environmental

Full Screen / Esc

Printer-friendly Version

Interactive Discussion

drivers, were revealed. With respect to total CH_4 emissions, neighboring chambers generally featured high differences in CH_4 fluxes, with no obvious trend along the transect. However, the spatial variability of diffusive CH_4 fluxes was characterized by lower emission rates near the shoreline and elevated fluxes at longer distances. These trends

5　might be a result of the increasing water column further from the shore, causing a reduced gas transfer across the air–water interface as a result of e.g. higher hydrostatic pressure to be overcome by gas bubbles on the one hand and an increased diffusive CH_4 flux based on enhanced CH_4 gradients on the other hand (Bastviken et al., 2004). In contrast, ebullative CH_4 emissions showed no gradient and were highly variable.

10　Thus, the detected spatial variability of total CH_4 emissions was dominated by highly variable ebullition events rather than by systematic differences in diffusive CH_4 emissions (Wik et al., 2011; Walter et al., 2008).

4　Conclusions

The results of the laboratory experiment, as well as the estimated relative contributions

15　of ebullition and diffusion during the field study, indicates that the presented algorithm for CH_4 flux calculation and separation into diffusion and ebullition delivers reasonable and robust results. Temporal dynamics, spatial patterns and relations with environmental parameters, well established in the scientific literature, such as soil temperature, water temperature gradients and wind velocity, became more pronounced when analyzed

20　separately for diffusive CH_4 emissions and ebullition. However, not all ebullition events (e.g. micro bubbles) seemed to be filtered correctly, as detected in case of enhanced CH_4 emissions during the beginning of August and the thereby superimposed diurnal cycling. Hence, further adaptation of measurement frequency and/or the applied data processing algorithm is required. In a next step, the flux separation algorithm should

25　be systematically tested against flux estimates generated with methods for measuring either ebullition or diffusion, such as bubble traps or bubble barriers. Moreover, the algorithm needs to be tested and evaluated with regards to generalizability and appli-

cability to other freshwaters and wetland ecosystems. Despite the mentioned short-comings, the presented calculation approach for separating CH_4 emissions increases the amount of information about the periodicity of CH_4 release and may help to reveal the influence of potential drivers as well as to explain temporal and spatial variability within both separated flux components.

References

Bastviken, D., Cole, J. J., Pace, M. L., and Tranvik, L. J.: Methane emissions from lakes: dependence of lake characteristics, two regional assessments, and a global estimate, Global Biogeochem. Cy, 18, 1–12, 2004.

Bastviken, D., Santoro, A. L., Marotta, H., Queiroz Pinho, L., Fernandes Calheiros, D., Crill, P., and Enrich-Prast, E.: Methane emissions from Pantanal, South America, during the low water season: towards more comprehensive sampling, Environ. Sci. Technol., 44, 5450–5455, 2010.

Bastviken, D., Tranvik, L. J., Downing, J. A., Crill, P. M., and Enrich-Prast, A.: Freshwater methane emissions offset the continental carbon sink, Science, 331, 50, 2011.

Chanton, J. P. and Whiting, G., J.: Trace gas exchange in freshwater and coastel marine environments: ebullition and transport by plants, in: Biogenic Trace Gases: Measuring Emissions from Soil and Water, edited by: Matson, P. A. and Hariss, R. C., Blackwell Science Ltd., UK, Chapter, 4, 98–125, 1995.

Christensen, T. R., Ekberg, A., Ström, L., Mastepanov, M., and Panikov, N.: Factors controlling large scale variations in methane emissions from wetlands, Geophys. Res. Lett., 30, 1–4, 2005.

Cole, J. J., Bade, D. L., Bastviken, D., Pace, M. L., and Van de Bogert, M.: Multiple approaches to estimating air-water gas exchange in small lakes, Limnol. Oceanogr., 8, 285–293, 2010.

DelSontro, T., Kunz, M. J., Kempter, T., Wüest, A., Wehrli, B., and Senn, D. B.: Spatial heterogeneity of methane ebullition in a large tropical reservoir, Environ. Sci. Technol., 45, 9866–9873, 2011.

Dengel, S., Zona, D., Sachs, T., Aurela, M., Jammet, M., Parmentier, F. J. W., Oechel, W., and Vesala, T.: Testing the applicability of neural networks as a gap-filling method using CH_4 flux data from high latitude wetlands, Biogeosciences, 10, 8185–8200, doi:10.5194/bg-10-8185-2013, 2013.

Deshmukh, C., Serça, D., Delon, C., Tardif, R., Demarty, M., Jarnot, C., Meyerfeld, Y., Chanudet, V., Guédant, P., Rode, W., Descloux, S., and Guérin, F.: Physical controls on CH_4 emissions from a newly flooded subtropical freshwater hydroelectric reservoir: Nam Theun 2, Biogeosciences, 11, 4251–4269, doi:10.5194/bg-11-4251-2014, 2014.

Goodrich, J. P., Varner, R. K., Frolking, S., Duncan, B. N., and Crill, P. M.: High-frequency measurements of methane ebullition over a growing season at a temperate peatland site, Geophys. Res. Lett., 38, 1–5, 2011.

Hahn-Schöfl, M., Zak, D., Minke, M., Gelbrecht, J., Augustin, J., and Freibauer, A.: Organic sediment formed during inundation of a degraded fen grassland emits large fluxes of CH_4 and CO_2, Biogeosciences, 8, 1539–1550, doi:10.5194/bg-8-1539-2011, 2011.

Hoffmann, M., Jurisch, N., Albiac Borraz, E., Hagemann, U., Drösler, M., Sommer, M., and Augustin, J.: Automated modeling of net ecosystem exchange based on periodic closed chamber measurements: a standardized conceptual and practical approach, Agr. Forest Meteorol., 200, 30–45, 2015.

Huttunen, J. T., Lappalainen, K. M., Saarijärvi, E., Väisänen, T., and Martikainen, P. J.: A novel sediment gas sampler and a sibsurface gas collector used for measurment of the ebullition of methane and carbon dioxide from a eutrophied lake, Sci. Total Environ., 266, 153–158, 2001.

IPCC: Summary for Policymakers, in: Climate Change, 2007: The Physical Science Basis, Contribution of Working Group I to the Fourth Assessment Report of the Intergovernmental Panel on Climate Change, edited by: Solomon, S., Qin, D., Manning, M., Chen, Z., Marquis, M., Av-

Title Page

Abstract | Introduction

Conclusions | References

Tables | Figures

◄ | ►

◄ | ►

Back | Close

Full Screen / Esc

Printer-friendly Version

Interactive Discussion

eryt, K. B., Tignor, M., and Miller, H. L., Cambridge University Press, Cambridge, United Kingdom and New York, NY, USA, 2007.

Juszczak, R. and Augustin, J.: Exchange of the greenhouse gases methane and nitrous oxide between the atmosphere and a temperate peatland in central Europe, Wetlands, 33, 895–907, 2013.

Koch, S., Jurasinski, G., Koebsch, F., Koch, M., and Glatzel, S.: Spatial variability of annual estimates of methane emissions in a Phragmites Australis (Cav.) Trin. Ex Steud. dominated restored brakish fen, Wetlands, 34, 593–602, 2014.

Koebsch, F., Jurasinski, G., Koch, M., Hofmann, J., and Glatzel, S.: Controls for multi-scale temporal variation in ecosystem methane exchange during the growing season of a permanently inudated fen, Agr. Forest Meteorol., 204, 94–105, 2015.

Koskinen, M., Minkkinen, K., Ojanen, P., Kämäräinen, M., Laurila, T., and Lohila, A.: Measurements of CO_2 exchange with an automated chamber system throughout the year: challenges in measuring night-time respiration on porous peat soil, Biogeosciences, 11, 347–363, doi:10.5194/bg-11-347-2014, 2014.

Lai, D. Y. F., Roulet, N. T., Humphreys, E. R., Moore, T. R., and Dalva, M.: The effect of atmospheric turbulence and chamber deployment period on autochamber CO_2 and CH_4 flux measurements in an ombrotrophic peatland, Biogeosciences, 9, 3305–3322, doi:10.5194/bg-9-3305-2012, 2012.

Lai, D. Y. F., Roulet, N. T., and Moore, T. R.: The spatial and temporal relationship between CO_2 and CH_4 exchange in a temperate ombotrophic bog, Atmos. Environ., 89, 249–259, 2014.

Limpens, J., Berendse, F., Blodau, C., Canadell, J. G., Freeman, C., Holden, J., Roulet, N., Rydin, H., and Schaepman-Strub, G.: Peatlands and the carbon cycle: from local processes to global implications – a synthesis, Biogeosciences, 5, 1475–1491, doi:10.5194/bg-5-1475-2008, 2008.

Maeck, A., Hofmann, H., and Lorke, A.: Pumping methane out of aquatic sediments – ebullition forcing mechanisms in an impounded river, Biogeosciences, 11, 2925–2938, doi:10.5194/bg-11-2925-2014, 2014.

Miller, L. G. and Oremland, R. S.: Methane efflux from the pelagic regions of four lakes, Global Biogeochem. Cy., 2, 269–277, 1988.

Ostrovsky, I., McGinnis, D. F., Lapidus, L., and Eckert, W.: Quantifying gas ebullition with echo sounder: the role of methane transport by bubbles in a medium-sized lake, Limnol. Oceanogr., 6, 105–118, 2008.

Title Page

Abstract | Introduction

Conclusions | References

Tables | Figures

|◀ | ▶|

◀ | ▶

Back | Close

Full Screen / Esc

Printer-friendly Version

Interactive Discussion

Prairie, Y. T. and del Giorgio, P. A.: A new pathway of freshwater methane emissions and the putative importance of microbubbles, Inland Waters, 3, 311–320, 2013.

Repo, M. E., Huttunen, J. T., Naumov, A. V., Chichulin, A. V., Lapshina, E. D., Bleuten, W., and Martikainen, P. J.: Release of CO_2 and CH_4 from small wetland lakes in western Siberia, Tellus B, 59, 788–796, 2007.

Sahlée, E., Rutgersson, A., Podgrajsek, E., and Bergstöm, H.: Influence from surrounding land on the turbulence measurments above a lake, Bound.-Lay. Meteorol., 150, 235–258, 2014.

Savage, K., Phillips, R., and Davidson, E.: High temporal frequency measurements of greenhouse gas emissions from soils, Biogeosciences, 11, 2709–2720, doi:10.5194/bg-11-2709-2014, 2014.

Schrier-Uijl, A. P., Veraart, A. J., Leffelaar, P. A., Berendse, F., and Veenendaal, E. M.: Release of CO_2 and CH_4 from lakes and drainage ditches in temperate wetlands, Biogeochemistry, 102, 265–279, 2011.

Tokida, T., Miyazaki, T., Mizoguchi, M., Nagata, O., Takakai, F., Kagemoto, A., and Hatano, R.: Falling atmospheric pressure as a trigger for methane ebullition from peatland, Global Biogeochem. Cy., 21, 1–8, 2007.

Van der Nat, F. W. and Middelburg, J.: Methane emission from tidal freshwater marshes, Biogeochemistry, 49, 103–121, 2000.

Walter, K. M., Chanton, J. P., Chapin III, F. S., Schuur, E. A. G., and Zimov, S. A.: Methane production and bubble emissions from arctic lakes: isotopic implications for source pathways and ages, J. Geophys. Res., 113, 1–16, 2008.

Walter, K. M., Smith, L. C., and Chapin III, F. S.: Methane bubbling from northern lakes: present and future contributions to the global methane budget, Phil. Trans. R. Soc. A, 365, 1657–1676, 2015.

Whiting, G. J. and Chanton, J. P.: Control of the diurnal pattern of methane emission from emergent aquatic macrophytes by gas transport mechnaisms, Aquat. Bot., 54, 237–253, 1996.

Wik, M., Crill, P. M., Varner, R. K., and Bastviken, D.: Multiyear measurements of ebullitive methane fluy from three subarctic lakes, J. Geophys. Res.-Biogeo., 118, 1307–1321, 2013.

Wik, M., Crill, P. M., Bastviken, D., Danielsson, A., and Norbäck, E.: Bubbles trapped in arctic lake ice: potential implications for methane emissions, J. Geophys. Res., 116, 1–10, 2011.

Title Page

Abstract | Introduction

Conclusions | References

Tables | Figures

|◄ | ►|

◄ | ►

Back | Close

Full Screen / Esc

Printer-friendly Version

Interactive Discussion

Wille, C., Kutzbach, L., Sachs, T., Wagner, D., and Pfeiffer, E.-M.: Methane emissions from Siberian artic polygonal tundra: eddy covariance measurements and modeling, Glob. Change Biol., 14, 1395–1408, 2008.

Yu, Z., Slater, L. D., Schafer, K. V. R., Reeve, A. S., and Varner, R. K.: Dynamics of methane ebullition from a peat monolith revealed from a dynamic flux chamber system, J. Geophys. Res., 119, 1789–1806, 2014.

Technical Note: A simple calculation algorithm to separate high-resolution

M. Hoffmann et al.

Title Page

Abstract | Introduction

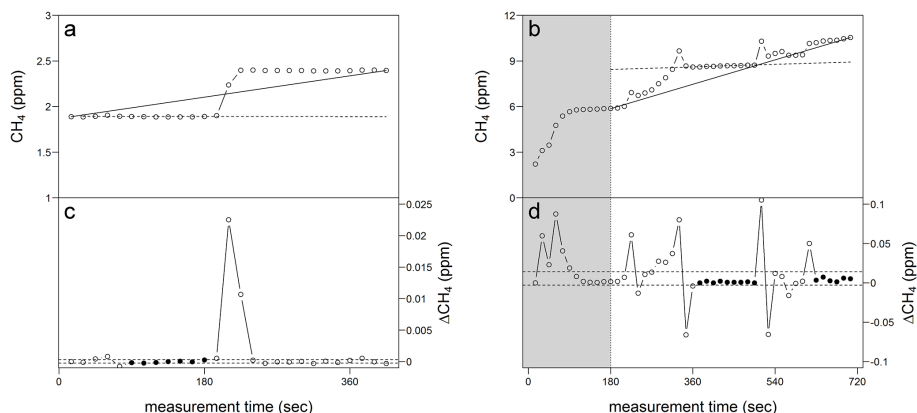Conclusions | References
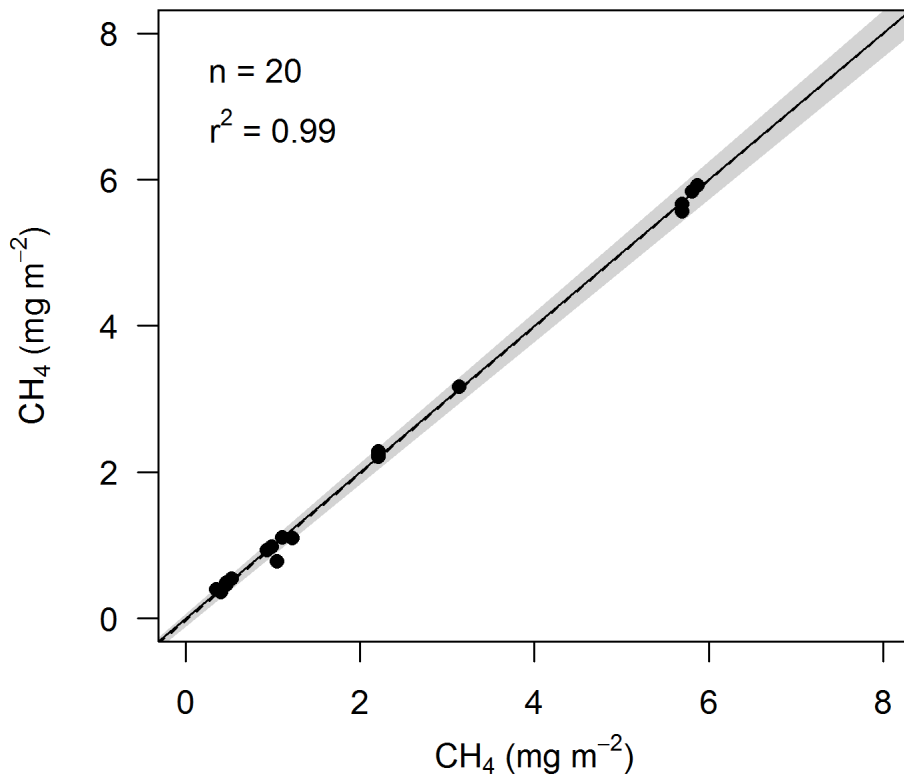
Tables | Figures

|◀ | ▶|

◀ | ▶

Back | Close

Full Screen / Esc

Printer-friendly Version

Interactive Discussion

Table 1. Monthly averages ± 1 standard deviation of hourly CH_4 emissions ($\mathrm{mg\,m^{-2}\,h^{-1}}$) for the chamber transect (from chamber I–IV, starting next to the shoreline). The median of standardized (beta) coefficients as well as of the Nash-Sutcliff's efficiency (NSE) based on daily linear and multiple linear regressions between different environmental drivers and calculated CH_4 emissions throughout the study period is shown below. Monthly averages as well as statistics are separated according to diffusion, ebullition and total CH_4 flux. Superscript numbers indicates significant differences between chambers. p values of applied linear and multiple linear regressions are indicated via asterisks.

Month	Chamber	$CH_{4\,diffusion}$	$CH_{4\,ebullition}$ $\mathrm{mg\,m^{-2}\,h^{-1}}$	$CH_{4\,total}$
July	I	$4.6^{24} \pm 3.1$	5.5 ± 7.0	$10.1^{24} \pm 7.8$
	II	$1.8^{134} \pm 1.5$	3.7 ± 6.9	$5.5^{134} \pm 7.1$
	III	$6.1^{24} \pm 4.0$	4.7 ± 6.9	$10.7^{24} \pm 8.2$
	IV	$8.7^{123} \pm 5.9$	4.7 ± 5.3	$13.3^{123} \pm 7.6$
August	I	5.1 ± 5.9	$5.0^{24} \pm 6.8$	10.1 ± 10.0
	II	3.7 ± 5.0	$2.9^{14} \pm 6.0$	6.5 ± 8.6
	III	5.7 ± 4.9	$5.8^{24} \pm 7.4$	11.5 ± 9.5
	IV	6.1 ± 6.8	$3.0^{13} \pm 5.0$	9.1 ± 9.4
September	I	$2.3^{24} \pm 2.0$	$1.8^{24} \pm 3.9$	$4.1^{24} \pm 4.8$
	II	$2.6^{1} \pm 2.7$	$1.1^{13} \pm 3.0$	$3.7^{13} \pm 4.4$
	III	$3.9^{4} \pm 3.9$	$5.4^{24} \pm 6.9$	$9.3^{24} \pm 8.8$
	IV	$1.3^{13} \pm 1.6$	$0.7^{13} \pm 3.4$	$2.1^{13} \pm 4.0$
Mean		5.1 ± 5.7	4.2 ± 6.5	9.2 ± 9.6

Driver	$CH_{4\,diffusion}$	$CH_{4\,ebullition}$	$CH_{4\,total}$
	median daily standardized (beta) coefficients		
wind velocity	-0.5	-0.1	-0.4
relative humidity (RH)	0.6^{*}	0.1	0.4
air temp. (2 m)	-0.6^{*}	-0.1	-0.4^{**}
water temp. (5 cm)	0.1^{**}	0.1	0.2
sediment temp. (2 cm)	0.3^{**}	0.0	0.2
Δ water-air temp.	0.6^{*}	0.1	0.4
median NSE of MLR	0.77	0.26	0.52

[1234] Significant difference ($\alpha = 0.1$) between chamber I (1), II (2), III (3) and IV(4).
[*] Significant dependency with median p value < 0.2 and [**] p value < 0.1.

Figure 1. Transect of automatic chambers (AC) established at the measurement site. The arrow indicates the position of the climate station near chamber II.
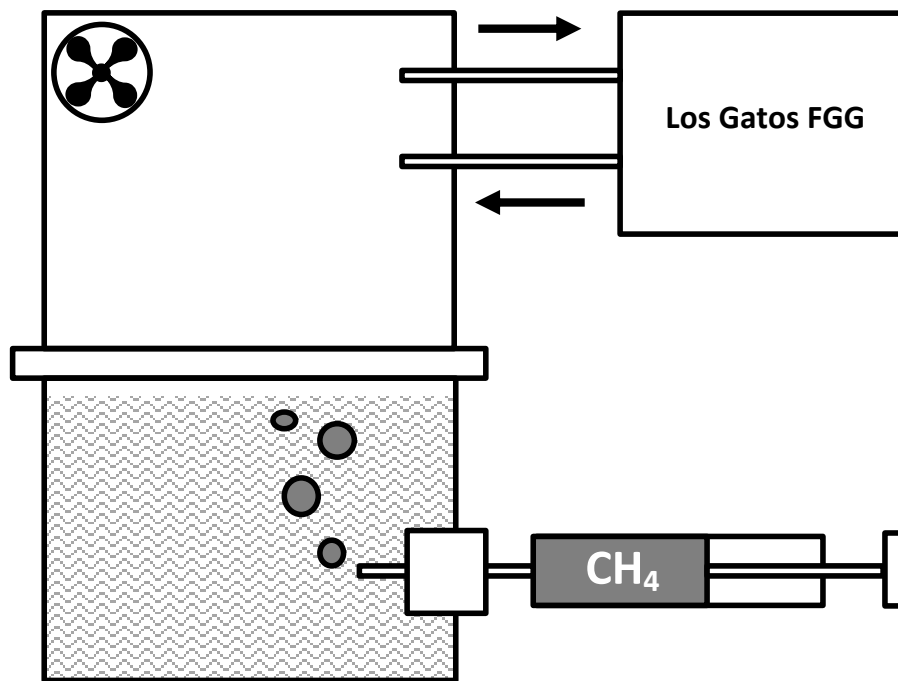
Figure 2. Scheme of experimental setup, used for simulation and determination of ebullition events. Crimped area represents water filled tub. Injections of gaseous mixture (25 000 ppm CH_4 within artificial air; Linde, Germany) amounted for 5, 10, 20, 30 and 50 mL.

Figure 3. Scatterplots of recorded concentrations (ppm) within chamber headspace for **(a)** simulated ebullition event and **(b)** exemplary CH_4 measurement. The respective total CH_4 emission rate is represented by the black solid line, whereas CH_4 released by diffusion is shown as a dashed line. The calculation of the corresponding diffusive flux is based on **(c–d)** concentration changes (ppm) between measurment points. Time spans dominated by diffusive CH_4 release are marked by black dots, enclosed by the 25 and 75 % quantiles ±0.25 IQR of obtained concentration changes, shown as black dashed lines. Unfilled dots outside the dashed lines display ebullition events (see also Goodrich et al., 2011; Miller and Oremland, 1988). Gray shaded areas indicate the applied deathband (field study) at the beginning of each measurement (25 %).

Full Screen / Esc

Figure 4. Scatterplot of amount of injected CH_4 and calculated corresponding CH_4 ebullition event. The solid black line indictes the 1 : 1 agreement. Linear fit between displayed values is represented by the black dashed line, and surrounded by the 95 % confidence interval (grey shaded area).
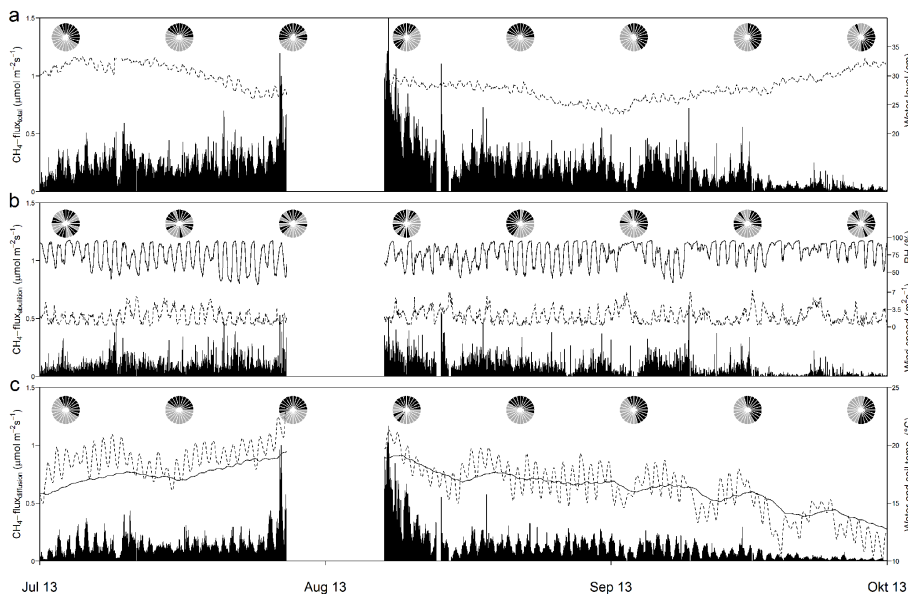
Figure 5. Time series of **(a)** total CH_4 emissions and corresponding amount of CH_4 released via **(b)** ebullition and **(c)** diffusion during the study period from July until September 2013. Development of important environmental parameters assumed to explain dynamics are shown next to it (**(a)** water level, **(b)** RH and wind speed and **(c)** soil (solid line) and water temperature (dashed line)). Pie charts represents the biweekly pooled diurnal cycle of measured CH_4 fluxes. Slices are applied clockwise, creating a 24 h clock, with black and light grey slices indicating hours with CH_4 flux above and below the daily mean, respectively.